Fuzzy Logic Based PI Closed Loop Control of Switched Reluctance Motor Drives Using Z-Source Inverter

Hari Prabhu.M
PG Scholar
Paavai college of Engineering
Anna University- Chennai

Mahendran.S
PG Scholar
Paavai college of Engineering
Anna University- Chennai

Rangarajan.V
PG Scholar
Paavai college of Engineering
Anna University- Chennai

Abstract

This paper is based on the redevelopment of control rule base,the fuzzy logic based PI controllers using Z-source inverter(ZSI) with output scaling factor(SF)self-tuning mechanism are proposed for application in the switched reluctance motor(SRM)drives.The aim of this paper is to simplify the program complexity of the controller by reducing the number of fuzzy sets of the membership functions(MFs) without losing the system performance and stability via the adjustable controller gain.ZSI exhibits both voltage-buck and voltage-boost capability. It reduces line harmonics,improves reliability,and extends output voltage range.The output SF of the controller can be tuned continuously by a gain updating factor,whose value is derived from fuzzy logic,with the plant error and error change ratio as input variables.Then the expected results,carried out on a four-phase6/4 pole SRM based on the dSPACEDS1104 platform, to show the feasibility and effectiveness of the devised methods and also performance of the proposed controllers will be compared with conventional counterpart.

1. Introduction

With the advances in power electronics and high-tech control techniques, as well as the development of high speed microcontrollers with powerful computation capability, switched reluctance motor (SRM) drives are under consideration in various applications requiring high performance, such as servomotor drives, electric vehicle propulsion, jet engine starter generators, etc. SRMs inherently feature numerous merits like simple and rugged structure, being maintenance free, high torque–inertia ratio, fault-tolerance robustness and reliability, high efficiency over a wide range of speeds, the capability to run in abominable circumstances, etc. [1].The requirements for variable-speed SRM drives include good dynamic and steady-state responses, minimum torque ripple, low-speed oscillation, and robustness. However, due to the heavy nonlinearity of the electromagnetic property and the coupling relationships among flux linkage, torque, and rotor position, it is not easy for an SRM to get satisfactory control characteristics. Therefore, new structure designs [2], [3], high performance magnetic cores [4] and adaptive control techniques [5],[6] in the innovation and improvement of various SRMs have been presented progressively in recent years.

When the exact analytical model of the controlled system is uncertain or difficult to be characterized, intelligent control techniques such as fuzzy logic control (FLC), neural network control, or genetic algorithm may allow better performance. Intelligent control approaches try to imitate and learn the experience of the human expert to get satisfactory performance for the controlled plant [7]. One of the most powerful tools that can translate linguistic control rules into practical operation mechanism is the FLC.Hence, the FLC is widely applied in a considerable variety of engineering fields today because of its adaptability and effectiveness [8]–[12]. It has been shown that fuzzy control can reduce hardware and cost and provide better performance than the classical PI, PD, or PID controllers [13],[14].Recently, fuzzy control theory has been widely studied, and various types of fuzzy controllers have also been proposed for the SRM to improve the drive performance further [8][9],[16]–[18]. In these research works, the main techniques utilized to enhance the self-adaptability and performance of the FLC are scaling factor (SF) tuning, rule base modification, inference mechanism improvement, and membership function redefinition and shifting. Among these techniques, SF tuning is the most used approach, and it has a significant impact on the performance of an FLC. The initial parameters and scaling gains of the controller are optimized by the genetic algorithm to minimize overshoot, settling time, and rising time. An adaptive fuzzy controller for torque-ripple minimization is presented by Mir *et al.* [9]. Aiming at torque-ripple minimization, the controller is independent from the accurate SRM model and can adapt to the change of motor characteristics. These characteristics include position

error robustness, avoidance of negative torque production, and torque-ripple minimization. This study was aimed at reducing the torque ripple and acoustic noise by an efficient fuzzy control algorithm. An adaptive FLC with scaling gain tuning is proposed in [17]. The universe of discourse (UOD) of the fuzzy sets can be tuned by altering the scaling gain according to the input variables. This significantly improves the system transient and steady-state responses. Koblara proposed a fuzzy logic speed controller for SRM drives [18]. This fuzzy controller, which is used in the outer loop, takes the speed error and change of error as the input signals to generate an equivalent control term. It can produce smooth torque and improve the system performance.Z-source inverter system for adjustable speed drives (ASD)[19][22].By controlling the shoot through duty cycle,it can produce any desired output ac voltage, even greater than the line voltage.It reduces line harmonics,and extends output voltage range.It is a relatively recent converter topology that exhibits both voltage-buck and voltage-boost capability[20].The control of a Z-source neutral point clamped inverter using the space vector modulation technique gives a better harmonic performance.ZSI is designed suitable for wind power conversion system[21].The main challenge in wind power system to maintain a constant voltage at the output with unpredictable variation in wind speed,is suitably taken care in steady state through buck-boost-capability of (ZSI). The most concerning disturbances affecting the quality of the power in the distribution system are voltage sag/swell[25].The ZSI uses an LC impedance grid to couple power source to inverter circuit and prepares the possibility of voltage buck and boost by short circuiting the inverter legs. Additionally a fuzzy logic control scheme for Z-source inverter based DVR is proposed to obtain desired injecting voltage.
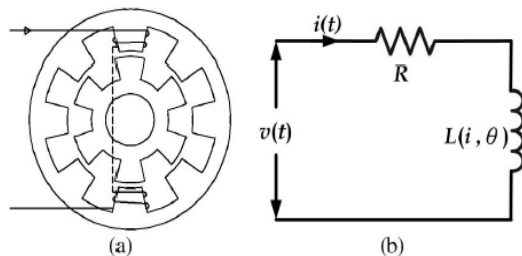

Figure 1.(a) Cross-sectional profile and (b)equivalent circuit of an 6/4-pole SRM

2. SRM drive system

2.1 SRM Behavior Model

In SRM, the torque is generated due to the push–pull between reluctance forces. The produced electromagnetic torque is related to the variation of the machine coenergy, and the coenergy varies with the flux linkage, excitation current, and rotor position. The flux linkage, inductance, and torque are highly coupled and nonlinear with the variation of rotor position and phase current, and hence, its magnetization characteristics and operating behavior are difficult to decouple and model mathematically. Fig. 1(a) and (b) shows the cross-sectional profile of a four-phase 6/4-pole SRM and the equivalent circuit of one phase winding, respectively. The equivalent circuit can be represented by a resistance R in series with an inductance L(i, θ), which is a function of rotor position θ and excitation current i. From Fig. 1(b), the phase voltage can be expressed by

$$V(t) = R.i(t) + \frac{d\lambda(i,\theta)}{dt} \qquad (1)$$

With

$$\lambda(i,\theta) = L(i,\theta)i \qquad (2)$$

Where λ is the flux linkage, which is dependent on i and θ. v(t), i(t), and L(i, θ) are the instantaneous voltage across the excited phase winding, the excitation current, and the self-inductance, respectively. According to (1) and (2), the dynamic behavior of the m-phase SRM can be denoted as

$$V_k = \sum_{j=1}^{m} \left\{ \left(R_k + \omega \frac{\partial Lkj}{\partial \theta} \right) ij + \left(Lkj + ij \frac{\partial Lkj}{\partial ij} \right) \frac{\partial ij}{\partial t} \right\}$$
$$k = 1,2,\ldots\ldots m \qquad (3)$$

where ω is the rotor angular velocity and m is the phase number.

The obtained coenergy is equal to the area enclosed by the λ−i curve over one excitation cycle and can be calculated by

$$W_{ce(i,\theta)} = \int_0^i \lambda(i,\theta)di \Big|_{\theta=constant} \qquad (4)$$

For a specified current, the induced electromagnetic torque can be obtained by differentiating the coenergy Wce with respect to the rotor position θ, which can be expressed as

$$T_{e(i,\theta)} = \frac{\partial W_{ce}(i,\theta)}{\partial \theta} \bigg|_{i=constant} \qquad (5)$$

Here, we define an incomplete torque function as

$$T_k = \frac{1}{2} \sum_{j=1}^{m} \{ sgn(k,j) i_j \frac{\partial L_{kj}}{\partial \theta} \}$$

$$k = 1,2,\ldots\ldots m \qquad (6)$$

Where

$$sgn(k,j) = \begin{cases} 1, & if \quad k = j \\ -1, & if \quad k \neq j \end{cases} \qquad (7)$$

From (2) and (4)–(7), including the mutual inductance, the produced totally electromagnetic torque can be denoted as

$$T_e = \sum_{k=1}^{m} i_k T_k \qquad (8)$$

The mechanical torque of the rotor can be expressed as

$$T_{mec} = T_e - B\omega - J\frac{d\omega}{dt} \qquad (9)$$

where *J*, *B*, and *T*mec stand for the machine's moment inertia, friction coefficient, and mechanical torque, respectively.

Together with (3), (6), (8), and (9), the matrix-form behavior model of the SRM, taking the magnetic coupling effect into account, can be denoted by (10),If the mutual inductance is negligible, then

$$\begin{cases} L_{kj} = 0, & if \quad k \neq j \\ L_{kj} \neq 0, & if \quad k = j \end{cases} \qquad (11)$$

2.2. Drive System Architecture

Shown in Fig. 2 is the configuration of the studied SRM drive system. It consists of four controllers, which include the fuzzy speed controller, the PI current controller, the exciting angle regulation controller, and the commutation logic controller; a gate driver circuit with photo couplers; a power inverter; and the four-phase 6/4-pole SRM. The fuzzy speed controller receives the speed error signal and converts it into four-phase current commands that will be sent to the current controller. The actual current, sensed by the Hall-effect sensor, is compared with the current command to obtain the current error. According to the error value, the pulse width modulation gating signals of insulated-gate bipolar transistors in an asymmetric half-bridge power inverter are generated by the current controller. The gating signals drive the power inverter through the photo coupler isolation. Z-source inverter system for adjustable speed drives(ASD)it can produce any desired output ac voltage,even greater than the line voltage.It reduces line harmonics,and extends output voltage range.ZSI exhibits both voltage-buck and voltage-boost capability. With the inputs of actual speed, speed errors, current, and rotor position, both algorithms of torque iterative learning control (TILC) and energy iterative learning control (EILC) are run to minimize the torque ripple and energy conversion loss by regulating the incremental turn-on and turn-off angles ($\Delta\theta$on,$\Delta\theta$off) and the duty cycle (*D*) to enhance the driving performance. When the speed error (ωerror) is acceptably low, the whole exciting angle regulation controller will be enabled to run the TILC and EILC processes and to compensate the parameter variations caused by the inaccurate motor model. The commutation logic controller is used to derive and determine the phase commutation moment according to the rotor position, excitation turn-on angle, and turn-off angle. In order to simplify the hardware complexity, all of the four controllers are implemented on a DSP-based dSPACE control platform.

$$
\begin{bmatrix} v_1 \\ v_2 \\ \vdots \\ v_m \\ T_{\mathrm{mec}} \end{bmatrix} =
\begin{bmatrix}
\left(R_1 + \omega\frac{\partial L_{11}}{\partial\theta}\right) & \omega\frac{\partial L_{12}}{\partial\theta} & \cdots & \omega\frac{\partial L_{1m}}{\partial\theta} & 0 \\
\omega\frac{\partial L_{21}}{\partial\theta} & \left(R_2 + \omega\frac{\partial L_{22}}{\partial\theta}\right) & \cdots & \omega\frac{\partial L_{2m}}{\partial\theta} & 0 \\
\vdots & \vdots & & \vdots & \vdots \\
\omega\frac{\partial L_{m1}}{\partial\theta} & \omega\frac{\partial L_{m2}}{\partial\theta} & \cdots & \omega\frac{\partial L_{mm}}{\partial\theta} & 0 \\
T_1 & T_2 & \cdots & T_m & -B
\end{bmatrix}
\begin{bmatrix} i_1 \\ i_2 \\ \vdots \\ i_m \\ \omega \end{bmatrix}
$$

$$
+ \begin{bmatrix}
\left(L_{11} + i_1\frac{\partial L_{11}}{\partial i_1}\right) & \left(L_{12} + i_2\frac{\partial L_{12}}{\partial i_2}\right) & \cdots & \left(L_{1m} + i_m\frac{\partial L_{1m}}{\partial i_m}\right) & 0 \\
\left(L_{21} + i_1\frac{\partial L_{21}}{\partial i_1}\right) & \left(L_{22} + i_2\frac{\partial L_{22}}{\partial i_2}\right) & \cdots & \left(L_{2m} + i_m\frac{\partial L_{2m}}{\partial i_m}\right) & 0 \\
\vdots & \vdots & & \vdots & \vdots \\
\left(L_{m1} + i_1\frac{\partial L_{m1}}{\partial i_1}\right) & \left(L_{m2} + i_2\frac{\partial L_{m2}}{\partial i_2}\right) & \cdots & \left(L_{mm} + i_m\frac{\partial L_{mm}}{\partial i_m}\right) & 0 \\
0 & 0 & \cdots & 0 & -J
\end{bmatrix}
\frac{d}{dt}\begin{bmatrix} i_1 \\ i_2 \\ \vdots \\ i_m \\ \omega \end{bmatrix} \quad (10)
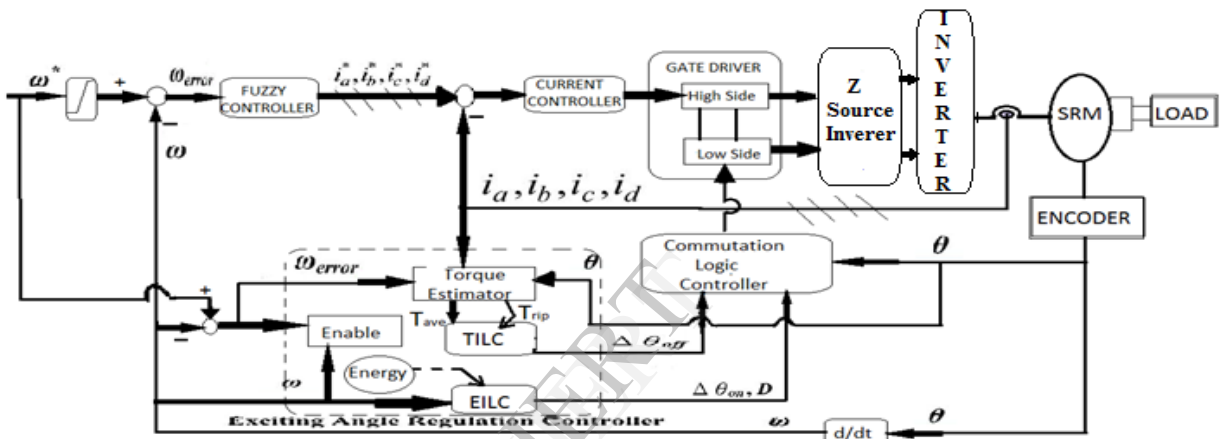$$

Figure 2. Architecture of the SRM drive system.

3. Fuzzy Logic Controller Design

In this section, the fuzzy control fundamentals will be outlined first, and then, the key point of self-tuning PI-like fuzzy controller (STFC) will be briefly reviewed. Afterward, the modified design of the proposed STFC will be described in detail.

Figure 3. Basic structure of a fuzzy logic control system

3.1 Fuzzy Control Philosophy

A basic FLC system structure, which consists of the knowledge base, the inference mechanism, the fuzzification interface, and the defuzzification interface, is shown in Fig. 3. Essentially, the fuzzy controller can be viewed as an artificial decision maker that operates in a closed-loop system in real time. It grabs plant output $y(t)$, compares it to the desired input $r(t)$, and then decides what the plant input (or controller output) $u(t)$ should be to assure the requested performance. The inputs and outputs are "crisp." The fuzzification block converts the crisp inputs to fuzzy sets, and the defuzzification block returns these fuzzy conclusions back into the crisp outputs.
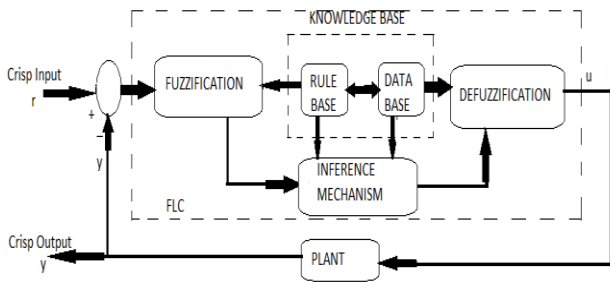
3.2 Overview of Self-Tuning FLC

The PI-like fuzzy controller (PIFC) is driven by a set of control rules rather than constant proportional and integral gains. The block diagrams

of a conventional PIFC and an STFC are shown in Figs. 4 and 5, respectively. The main difference between both controllers is that the STFC includes another control rule base for the gain updating factor α [14]. Adaptability is necessary for fuzzy controllers to ensure acceptable control performance over a wide range of load variations regardless of inaccurate operating knowledge or plant dynamic behaviour. There are three commonly used methods to make a fuzzy controller adaptive: input or output SF tuning, MF definition or shifting, and control rule modification. In a classical fuzzy controller, the UOD tuning of the MFs of the input or output variables can be used to overcome the steady-state error. Here, a discrete-time controller with two inputs and a single output is considered. From Fig. 5, the error e and change of error Δe are used as the input variables, which are defined as,

$$e(k) = r(k) - y(k) \qquad (12)$$

$$\Delta e(k) = e(k) - e(k-1)$$
$$= y(k-1) - y(k)$$
$$\text{if } r(k) = r(k-1) \qquad (13)$$

where r and y denote the reference command and plant output, respectively. Indices k and k−1 represent the current and previous states of the system, respectively. The controller output is the incremental change of the control signal $\Delta u(k)$. The control signal can be obtained by

$$u(k) = u(k-1) + \Delta u(k). \qquad (14)$$

The UOD in all membership functions of the controller inputs, i.e., e and Δe, and output, i.e., Δu, are defined on the normalized domain [−1, 1], as shown in Fig. 6. The linguistic values NB, NM, NS, ZE, PS, PM, and PB stand for negative big, negative medium, negative small, zero, positive small, positive medium, and positive big, respectively. Then, the UOD for the gain updating factor α (which is utilized to fine tune the output SF) is normalized over the interval [0, 1], as shown in Fig. 7. The linguistic values ZE, VS, S, SB, MB, B, and VB represent zero, very small, small, small big, medium big, big, and very big, respectively. Here, except for the two fuzzy sets at the outmost ends (trapezoidal MFs are considered), symmetric triangles with equal bases and 50% overlap with adjacent MFs are chosen. The SFs Ge, $G\Delta e$, and $G\Delta u$, which perform the specific normalization of input and output variables, play a role equivalent to that of the gains of a conventional controller. Hence, they hold the dominant impact on controller stability and performance.
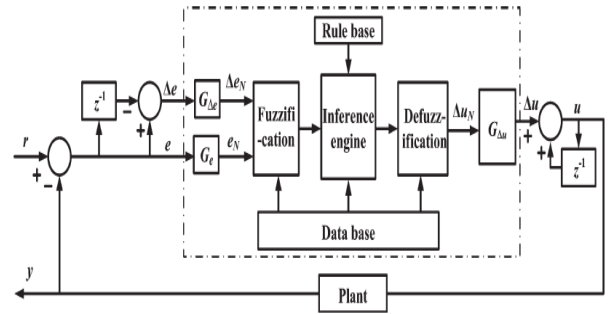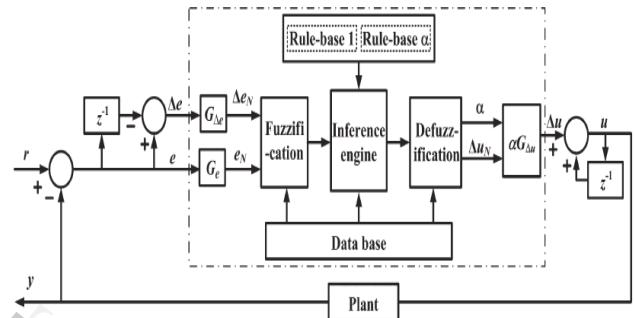

Figure 4. Block diagram of a conventional PIFC.

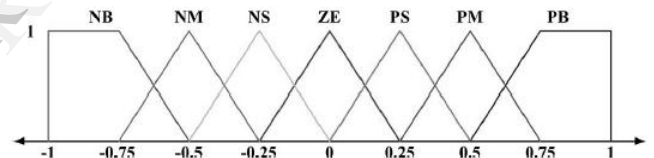Figure 5. Block diagram of an STFC

Figure 6. Membership functions of e, Δe, and Δu.
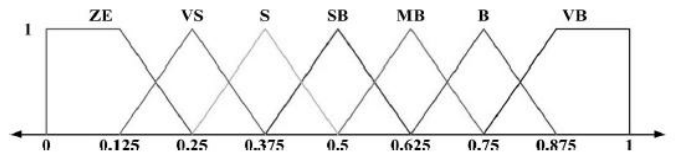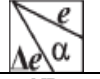

Figure 7. Membership function of the gain updating factor α.

"Table 1. Rule Base for deriving **ΔU**".

$\Delta e \backslash \alpha$ e	NB	NM	NS	ZE	PS	PM	PB
NB	NB	NB	NB	NM	NS	NS	ZE
NM	NB	NM	NM	NM	NS	ZE	PS
NS	NB	NM	NS	NS	ZE	PS	PM
ZE	NB	NM	NS	ZE	PS	PM	PB
PS	NM	NS	ZE	PS	PS	PM	PB
PM	NS	ZE	PS	PM	PM	PM	PB
PB	ZE	PS	PS	PM	PB	PB	PB

"Table 2. Rule Base for deriving **α**".

e / Δe	NB	NM	NS	ZE	PS	PM	PB
NB	VB	VB	VB	B	SB	S	ZE
NM	VB	VB	B	B	MB	S	VS
NS	VB	MB	B	VB	VS	S	VS
ZE	S	SB	MB	ZE	MB	SB	S
PS	VS	S	VS	VB	B	MB	VB
PM	VS	S	MB	B	B	VB	VB
PB	ZE	S	SB	B	VB	VB	VB

Figure 8. Block diagram of the proposed FLC with a reduction of the control rule.

The MFs for both normalized inputs (*eN* and Δ*eN*) and output (Δ*uN*) of the controller have been defined on the normalized domain [−1, 1].For conventional FLCs, the controller output (Δ*uN*) is mapped onto the respective actual output (Δ*u*) domain by the output SF $G_{\Delta u}$. On the other hand, the actual output of the self tuning FLC is obtained by using the effective SF $\alpha G_{\Delta u}$ [14]. Hence, adjusting the SFs can modify the corresponding UODs of the control variables. The adequate values of the input and output SFs can be derived based on the professional experience from the plant under control. It can also be derived through trial and error to achieve the best acceptable control performance. As shown in Fig. 5, the relationships between the SFs and the input and output variables of the STFC can be expressed as follows:

$$e_N = G_e e \tag{15}$$

$$\Delta e_N = G_{\Delta e} \Delta e \tag{16}$$

$$\Delta u = (\alpha G_{\Delta u}) \Delta u_N \tag{17}$$

The rule bases for computing controller output Δ*u* and gain updating factor *α* are shown in Tables I and II, respectively. This is a commonly used rule base designed with a 2-D phase plane. The control rules, shown in Tables I and II, are built based on the characteristics of the step response. For example, if the output is falling far away from the command, a large control signal that pulls the output toward the command is expected, whereas a small control signal is required when the output is near and approaching the steady state. The rule forms used for Δ*u* and *α* can be described, respectively, by

RΔu : If e is E and Δe is ΔE, then Δu is ΔU
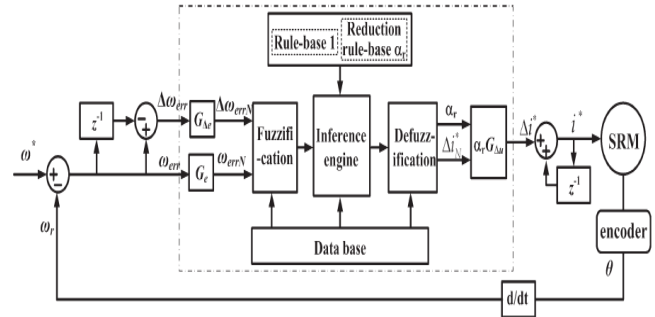Rα : If e is E and Δe is ΔE, then α is **α**.

3.3 Self-Tuning FLC With Control Rule Reduction

This work presents a simple but robust model-independent self-tuning mechanism for FLCs with the most important feature that it depends neither on the process being controlled nor on the controller used. The control algorithm must be implemented on the microcontroller with limited memory space and computational capability. The rule base of the STFC proposed in [14] chose seven fuzzy sets for each membership function of the input variables *e* and Δ*e*. Forty-nine fuzzy rules are needed for deriving controller output Δ*u* and *α*, respectively. This is a challenge to the performances of the used DSP or micro-controller unit. This paper focuses on, first, the reduction of the number of fuzzy rules for deriving *α* and, second, the simplification of the memory requirement and computational complexity of the designed controller. The architecture of the proposed controller with control rule reduction is shown in Fig. 8. Here, speed error ω_{err} and change of error $\Delta\omega_{err}$ are selected as input variables, and the output variable is the current command Δ*i**. The modifications of the devised controller on the aforementioned STFC are described as follows.

3.3.1 Membership Function Selection The MFs of controller output Δ*i**, as shown in Fig. 6, are the same as the definition of Δ*u*, and its range of UOD is normalized on [−1, 1].The MFs of ω_{err} and $\Delta\omega_{err}$ can be briefly divided into three categories, i.e., speed error (or error change rate) is negative (N), zero (ZE), and positive (P).
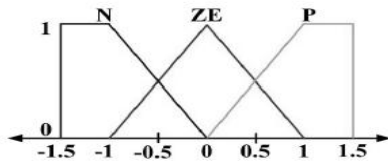
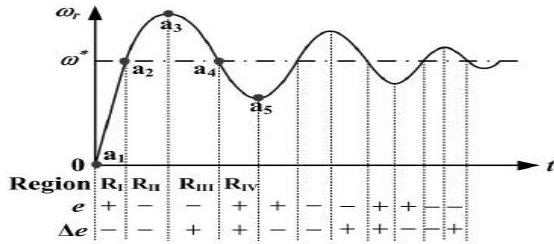Figure 9. MFs of ωerr and $\Delta\omega$err.

Figure 10. Dynamic behavior of motor step response.

Hence, three fuzzy sets for error and error change rate are chosen here, as shown in Fig. 9. Similarly, the MFs of gain updating factor αr are defined with three fuzzy sets, i.e., small (S), medium (M), and big (B), but with different domains for different operating points. This is to take the high nonlinearity of the SRM into consideration, obtain good control resolution, and provide better adaptability to set-point changes.

3.3.2 Rule Base Derivation The rule base for deducing the incremental change of controller output Δi^* is the same as that shown in Table I. Here, the focus is on the reduction of rule numbers for deriving updating factor αr. To reduce the rule numbers of Table II, a practical observation of the motor step response, as shown in Fig. 10. The speed response can be roughly divided into four regions, i.e., RI−RIV, and two sets of particular points, i.e., crossover points ($a2$, $a4$) and peak points ($a3$, $a5$). According to the definitions of (12) and (13), the signs of e and Δe will change when the response curve passes through the different regions. For example, the sign of ($e,\Delta e$) in regions RII and RIV are $(−,−)$ and $(+, +)$, respectively. The states in these two regions mean that the speed now is not only upward (RII) or downward (RIV) far away from the speed command but is also going farther away from it. In this situation, the controller should provide large gain ($\alpha rG\Delta u$) to prevent worsening the condition. This can be realized by the following rules: If both error and change of error are negative (or positive), then αr is big. On the other hand, when the state is near the speed command and is moving nearer toward it, the response curve in this situation is located on region RI or RIII, and the sign of ($e,\Delta e$) is opposite. At this

time, the controller should make the gain small to avoid overshoot or undershoot and reduce the settling time. The rule can be formed as follows: If the error and change of error are of opposite signs, then αr is small. In addition, when the state is close to the steady state, i.e., either e or Δe is zero, which means that the response has just reached or left the set point but is moving away upward or downward from the set point rapidly. In this situation, medium gain will prevent overshoot or undershoot. This can be accomplished by the following rule: If either the error or the change of error is zero, then αr is medium. This type of gain variation around the speed command will also avoid excessive oscillation and increase convergence rate. Finally, at the steady state, the controller should provide very small gain to prevent the chattering problem around the set point. The rule for this condition is as follows: If both the error and change of error are zero, then αr is small. Consequently, based on the understanding and deduction of response behaviour and the rule base of α (Table II), the proposed frame of the reduced rule base for deriving αr is shown in Table III. In this proposed scheme, although there are 45 control rules (nine basic rules for αr $\times$ 5 steps shifting) programmed and the total rule number (45 for αr and 49 for Δi^*) saved in the memory is 94, in practical cases when the control process is running, according to the speed command, the program will be switched to run a subroutine, which is instructed to correspond to one of the five speed command ranges. Each time, only nine control rules are used to derive αr when the chosen subroutine is executed. Consequently, when the control procedure is running, the numbers of control rules used to derive Δi^* and αr are 49 and 9, respectively, and the decrease in rule numbers compared with STFC is 40.

Table 3. Rule Base Frame for deriving αr

$\Delta\omega_{err}$ \ α_r \ ω_{err}	NB	NM	NS	ZE	PS	PM	PB
NB	VB	VB	VB	a_2	SB	S	ZE
NM	VB	B	B	M	MB	S	VS
NS	R_{II} (-e, -Δe)		VB		R_I (+e, -Δe)		VS
ZE	S a_3	M	MB	S	MB	M a_1, a_5	
PS	VS	S	VS	VB	B	MB	VB
PM	VS	S	MB	M	B	B	VB
PB	R_{III} (-e, +Δe)	B	a_4		R_{IV} (+e, +Δe)		

3.4. Self-Tuning FLC With Combined Rule Base

In order to further reduce the numbers of control rules to simplify the complexity of the controller, another modified rule base with fewer control rules, which integrates the rule base of controller output (Δu) with the gain updating factor (α) rule base, is devised. The controller output gain can be tuned continuously with the updating factor αi, it is integrated and embedded into the combined rule base. The principle of how to combine the two rule bases are described as follows:

As the aforementioned exploration for the step response of the SRM is shown in Fig. 10, integrating the two rule bases into a union rule base to simplify the system is feasible. The basic principles and the design guidelines are explained as follows:

1) A different linguistic value of the controller output should be defined for each distinct combination of linguistic values for Δu and α, as shown in Tables I and II. For example, when e is PB and Δe is NS, then Δu is PM (Table I) and α is VS (Table II), so the pair (PM, VS) forms a distinct combination. From the linguistic pair (PM, VS), we deduce that the trend of controller output should be positive small, i.e., a control rule can be defined as follows: If e is PB and Δe is NS, then the combined output $\Delta u\alpha i$ is PS. Using the same principle, the rule bases of Δu and α can be integrated into a modified combined rule base, as shown in Table IV.

2) In some situations, it is observed that if e is NS and Δe is PB, then Δu is PS and α is SB, so the pair (PS, SB) forms another distinct combination.

Table 4. Rule Base for $\Delta i*\alpha i$ derivation

ω_{err} / $\Delta\omega_{err}$ Δi_α	NB	NM	NS	ZE	PS	PM	PB
NB	NB	NB	NB	NS	NVS	NVS	ZE
NM	NB	NM	NS	NS	NVS	ZE	PVS
NS	NB	NS	NVS	NVS	ZE	PS	PS
ZE	NS	NS	NVS	ZE	PVS	PS	PS
PS	NS	NS	ZE	PVS	PVS	PS	PB
PM	NVS	ZE	PVS	PS	PS	PM	PB
PB	ZE	PVS	PVS	PS	PB	PB	PB

From the linguistic pair (PS, SB), it can be inferred that the controller output trends toward positive very small, i.e., we can define a control rule as follows: If e is NS and Δe is PB, then the combined output $\Delta u\alpha i$ is PVS. On the other hand, when e is PM and Δu is NB, then Δu is NS and α is S, forming the linguistic

pair (NS, S). Thus, it can be said that the controller output trends toward negative very small, i.e., we can define a control rule as follows: If e is PM and Δe is NB, then the combined output $\Delta u\alpha i$ is NVS. When the PVS and NVS are new linguistic values, they must be redefined and added to a new MF, as shown in Fig. 11.
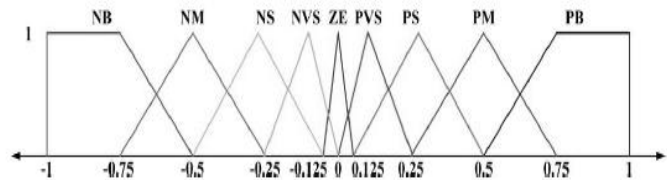

Figure 11. Membership functions of combined output $\Delta u\alpha i$.

3) Owing to the highly nonlinear controller output that is dependent not only on the rule base but also on its neighbouring rules in the rule base. From Fig. 11, in order to enhance the sensitivity and resolution of the controller and take nonlinearity into account, the fuzzy sets of the $\Delta u\alpha i$ MFs in the vicinity of ZE are more concentrated than in the other ranges. The range adjustment or shifting of UOD nearby the set point will prevent system response from excessive oscillation and increase the convergence rate of the response to the steady state.

An STFC with a modified union rule base is developed. The controller block diagram is shown in Fig. 12. The controller output $\Delta u\alpha i$ can be tuned continuously online with the assistance of the updating factor αi. The updated law is based on the union rule base shown in Table IV. The combined rule base was derived from integrating Tables I and II and replacing two new linguistic values PVS and NVS. The Mamdani-type inferential method cooperating with the center-of-area defuzzification procedure is utilized to produce the crisp controller output.

3.5 Gain Tuning Strategy

The PIFC without scaling gain tuning mechanism has a drawback, i.e., as the controller design is finished, the defined domain of the input and output variables is fixed. This may result in long settling time and oscillation around the preset speed when the system approaches the steady state. This is caused by low controller resolution when the speed error is small. In order to obtain satisfactory performance, the UOD of the controller should be adjusted according to the operating point. Therefore, the fuzzy controller, which can change UOD by tuning scaling gains through a continuous and

nonlinear variation of the updating factor, is developed. Here, the attention is focused on the tuning of output scaling gain because it is equivalent to the controller gain, and output-gain regulation plays a dominant role due to its strong impact on the overall performance of the controller. The self-adjusting mechanism of the proposed fuzzy controllers is described as follows.

3.5.1. Variation Effect of Input and Output SFs

SF modulation is one of the most employed solutions to enhance the performance of a fuzzy controller. The design of the SFs, particularly the output SF, is very crucial in an FLC because of their influences on the performance. Take the STFC shown in Fig.5 as an example. Converting e, Δe, and Δu into eN, ΔeN, and ΔuN by the scaling gains, respectively, means that they are transferred from the actual UOD into the interval $[-1, 1]$ (normalization).The effect of SF adjustment is equivalent to extending or shrinking the actual UOD of the input and output variables.

3.5.2 Self-Tuning Mechanism

The systemic methods for gain tuning to obtain the optimal response because the determination of the optimal values of the adjustable parameters requires the knowledge of a precise model of the plant. Moreover, the practical testing results show that the effect of input SF tuning has lesser impact on system performance than output SF tuning, and both types of SF tuning will increase the system complexity further. Therefore, only output SF tuning is adopted in the proposed two modified STFCs. The design guidelines are described as follows:

Step 1. Set αr or αi as 1.0 (without gain tuning), and obtain the most suitable values of Ge, $G\Delta e$, and $G\Delta u$ using the simple method [18]. For the proposed two FLCs, the proper initial values of Ge, $G\Delta e$, and $G\Delta u$ can be obtained by (18) for control rule reduction and (19) for the combined rule base, respectively. Choosing Ge $G\Delta e$ and $G\Delta u$ to cover the whole normalized domain $[-1, 1]$ or interval $[emin, emax]$. An appropriate initial operating condition is obtained when a good transient response is achieved.

$$Ge = \frac{1}{\omega err,max} \ (or \ \frac{1}{|\omega err,min|})$$

$$G\Delta e = \frac{1}{\Delta \omega err,max} \quad G\Delta u = \Delta umax \qquad (18)$$

$$Ge = \frac{\omega err,max}{\omega err} \ (or \ \frac{|\omega err,min|}{\omega err})$$

$$G\Delta e = \frac{\Delta \omega err,max}{\Delta \omega err} \quad G\Delta u = \frac{\Delta u}{\Delta u max} \qquad (19)$$

Step 2. Keep the values of Ge, $G\Delta e$, and $G\Delta u$ the same as those in Step 1), and begin to tune the updating factor. In this step, the controller output and updating factor can be expressed by (20) and (21), respectively, where $\alpha index$ is αr or αi represents the updating factor for the FLC with control rule reduction or combined rule base. $f\alpha$ index is a nonlinear function defined on the e and Δe planes, and $k\Delta u$ is the scaling constant of $G\Delta u$. Here, $G\Delta u$ is set $k\Delta u$ times greater than that obtained in Step 1). The determination of $k\Delta u$ is empirical. For example, if the system is required to keep tracking the command without any overshoot, $k\Delta u$ can be set small to get a smaller output. At the same time, the output SF can be fine-tuned by altering the value of $\alpha index$ to achieve a relatively small but satisfactory output.
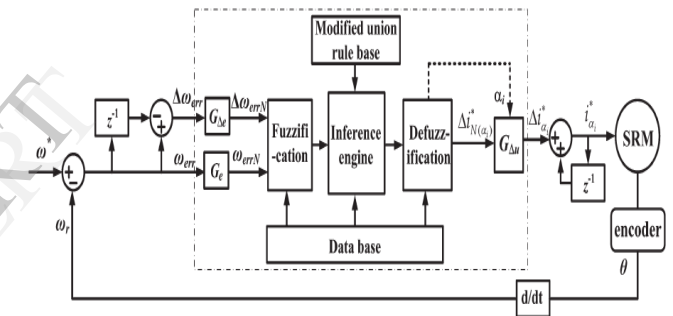

Figure 12. Block diagram of the proposed FLC with union rule base.

On the other hand, if we want to shorten the rise time, the $k\Delta u$ in (20) should be set larger. A large value of $k\Delta uG\Delta u$ is utilized in the proposed schemes to counteract the effect that α always lies in $[0, 1]$ and guarantee a faster response with relatively small overshoot

$$\Delta u(k) = \alpha index(k)(k\Delta uG\Delta u)\Delta uN \qquad (20)$$

$$\alpha index(k) = f\alpha index(e(k),\Delta e(k)) \qquad (21)$$

Step 3. Fine-tune the rules for $\alpha index$ based on the required response and the particular considerations for deriving the control rules if necessary. Hence,the proper $\alpha index$ is fine-tuned from various operating conditions.

Finally, the performance will be compared to shows that the STFC with rule reduction is the best among the three, but it is close fought to the STFC with combined rule base, and also demonstrates that the proposed controller can quickly regulate itself to adapt to the current environmental change.

4. Conclusion

In this paper, thus the modified fuzzy logic based PI controllers using Z-source inverter with gain self-tuning mechanism by altering a gain updating factor has been devised for the SRM drive system. The modified rule bases are designed to simplify the program complexity of the controller by reducing the number of fuzzy sets of the membership functions without losing the system performance and stability using the adjustable controller gain. Z-source inverter,that exhibits both voltage-buck and voltage-boost capability.It reduces line harmonics, improves reliability,and extends output voltage range. Both rule bases are based on the fuzzy control rules, which are derived from the practical understanding of the SRM's basic behaviour,operating experience. Here, attention is focused on the adjustment of the output SF because output-gain regulation has higher impact on the performance and stability of the system and the proposed controller can also simplify the complexity of the control system.Based on the dSPACE DS1104 platform, tests on a four-phase 6/4-pole SRM under the speed set-point change and load disturbance have been carried out to measure various performance indices such as peak overshoot or undershoot, steady-state error, rise time, settling time, etc.The expected results of the proposed control, shows very good stability and robustness against speed and load variations over a wide range of operating conditions and also the performance of the proposed controllers will be compared with conventional PIFC.

References

[1] T. J. E Miller, *Electronic Control of Switched Reluctance Machines*. London, U.K.: Oxford Univ. Press, 2001.

[2] J. G. Amoros and P. Andrada, "Sensitivity analysis of geometrical parameters on a double-sided linear switched reluctance motor," *IEEE Trans. Ind. Electron.*, vol. 57, no. 1, pp. 311–319, Jan. 2010.

[3] P. C. Desai, M. Krishnamurthy, N. Schofield, and A. Emadi, "Novel switched reluctance machine configuration with higher number of rotor poles than stator poles: Concept to implementation," *IEEE Trans. Ind. Electron.*, vol. 57, no. 2, pp. 649–659, Feb. 2010.

[4] J. Corda and S. M. Jamil, "Experimental determination of equivalent circuit parameters of a tubular switched reluctance machine with solid-steel magnetic core," *IEEE Trans. Ind. Electron.*, vol. 57, no. 1, pp. 304–310, Jan. 2010.

[5] H. Abootorabi Zarchi, J. Soltani, and G. Arab Markadeh, "Adaptive input–output feedback-linearization-based torque control of synchronous reluctance motor without mechanical sensor," *IEEE Trans. Ind. Electron.*, vol. 57, no. 1, pp. 375–384, Jan. 2010.

[6] T. Orlowska-Kowalska, M. Kaminski, and K. Szabat, "Implementation of a sliding-mode controller with an integral function and fuzzy gain value for the electrical drive with an elastic joint," *IEEE Trans. Ind. Electron.*, vol. 57, no. 4, pp. 1309–1317, Apr. 2010.

[7] P. Vas, *Artificial-Intelligence-Based Electrical Machines and Drives: Application of Fuzzy, Neural, Fuzzy-Neural, and Genetic- Algorithm-Based Techniques*. London, U.K.: Oxford Univ. Press, 1999.

[8] M. Chen, Q. Sun, and E. Zhou, "New self-tuning fuzzy PI control of a novel doubly salient permanent-magnet motor drive," *IEEE Trans. Ind. Electron.*, vol. 53, no. 3, pp. 814–821, Jun. 2006.

[9] S. Mir, M. E. Elbuluk, and I. Husain, "Torque-ripple minimization in switched reluctance motors using adaptive fuzzy control," *IEEE Trans. Ind. Appl.*, vol. 35, no. 2, pp. 461–468, Mar./Apr. 1999.

[10] T. Orlowska-Kowalska, M. Dybkowski, and K. Szabat, "Adaptive sliding mode neuro-fuzzy control of the two-mass induction motor drive without mechanical sensors," *IEEE Trans. Ind. Electron.*, vol. 57, no. 2, pp. 553–564, Feb. 2010.

[11] M. N. Uddin and M. A. Rahman, "High-speed control of IPMSM drives using improved fuzzy logic algorithms," *IEEE Trans. Ind. Electron.*, vol. 54, no. 1, pp. 190–199, Feb. 2007.

[12] M. A. Fnaiech, F. Betin, G. A. Capolino, and F. Fnaiech, "Fuzzy logic and sliding-mode controls applied to six-phase induction machine with open phases," *IEEE Trans. Ind. Electron.*, vol. 57, no. 1, pp. 354–364, Jan. 2010.

[13] Y. Zhao and E. G. Collins, Jr., "Fuzzy PI control design for an industrial weigh belt feeder," *IEEE Trans. Fuzzy Syst.*, vol. 11, no. 3, pp. 311–319, Jun. 2003.

[14] R. K. Mudi and N. R. Pal, "A robust self-tuning scheme for PI- and PD type fuzzy controllers," *IEEE Trans. Fuzzy Syst.*, vol. 7, no. 1, pp. 2–16, Feb. 1999.

[15] A. G. Perry, G. Feng, Y. F. Liu, and P. C. Sen, "A design method for PI-like fuzzy logic controller for DC–DC converter," *IEEE Trans. Ind. Electron.*, vol. 54, no. 1, pp. 190–199, Feb. 2007.

[16] S. Chowdhuri, S. K. Biswas, and A. Mukherjee, "Performance studies of fuzzy logic based PI-like controller designed for speed control of switched reluctance motor," in *Proc. IEEE Int. Conf. Ind. Electron. Appl.*, 2006, pp. 1–5.

[17] J. Xiu and C. Xia, "An application of adaptive fuzzy logic controller for switched reluctance motor drive," in *Proc. IEEE Fuzzy Syst. Knowl. Disc.*, 2007, pp. 154–158.

[18] T. Koblara, "Implementation of speed controller for switched reluctance motor drive using fuzzy logic," in *Proc. OPTIM*, 2008, pp. 101–105.

[19] Fang Z. Peng, Xiaoming Yuan, Xupeng Fang, and Zhaoming Qian, "Z-Source Inverter for Adjustable Speed Drives," ," *IEEE Trans. Power Electron.,* vol.1, no. 2,pp.33-35, June 2003.

[20] Francis Boafo Effah, Patrick Wheeler, Jon Clare, and Alan Watson, "Space-Vector-Modulated Three-Level Inverters With a Single Z-Source Network," *IEEE Trans. PowerElectron.,*vol.28,no.6,pp.2806-2815,June2013.

[21] Santosh sonar and Tanmoy maity, "Z-source Inverter based control of Wind Power," presented at the IEEE Industry Applications Soc. Annu. Meeting, 2011.

[22] Fang Zheng Peng,Alan Joseph, JinWang, Miaosen Shen, Lihua Chen, Zhiguo Pan, Eduardo Ortiz-Rivera, and Yi Huang, "Z-Source Inverter for Motor Drives," *IEEE Trans. Power Electron.,* vol.20, no. 4,pp.857-863, July 2005.

[23]M.Balamurugan, T.S. Sivakumaran, and M.Aishwariya Devi,"Voltage Sag/Swell Compensation Using Z-source Inverter DVR based on FUZZY Controller," presented at IEEE International Conference on Emerging Trends in Computing, Communication and Nanotechnology, pp.648-653 ,2013.